Approximating Geometry of Unknown Particles from Coupled Brownian Motion in Optical Tweezers

Authors: Liu Yi, Isaac Godoy, Emily Rush, Lyuna Niemet

Advisor: Conall McCabe

BACKGROUND INFORMATION

Brownian motion is described by the random motion of particles suspended in a fluid (liquid or a gas), resulting from their collision with the fast-moving atoms or molecules in the fluid.

Optical tweezers are optical laser instruments that trap particles and microscopic objects with forces at a focal point in their beams shown in Figure 1. These restorative forces counteract Brownian motion using the conservation of momentum in photons fired in each beam of light. This only works because of the scale, with smaller particles introducing more irregularity in the restoring forces.

The use of optical tweezers is extremely helpful in biophysics! Many use these instruments to hold bacteria, microscopic cells, and DNA in place to manipulate them.

Fig 1: Experimental configuration to observe thermal force fluctuations in a DNA molecule using optical tweezers. Adapted from [1].

RESEARCH QUESTION

Is it possible to approximate the geometry of an unknown particle from its averaged Brownian trajectory in an optical tweezer?

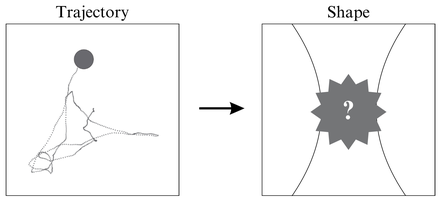

We hypothesize that it is possible to extrapolate information about a particle's geometry from its averaged Brownian trajectory. However, as the geometric complexity of the unknown particle increases, the percentage error of the estimate will also increase.

To test this hypothesis, we constructed and validated a general model for an asymmetric particle in an optical trap using Python, split into blinded sub-teams to encode and estimate geometry-induced parameters, and evaluated how estimation error changed with respect to a calibrated geometric complexity measure.

OPTICAL TRAP EQUATION

The equation used above [1] is meant to represent the instantaneous velocity at any point in time, given by the derivative of the position vector. Here, our gamma term represents the particle's friction coefficient, a constant 'dampening' value. Here, this is essentially the amount of resistance that the particle experiences being in a medium, where a higher gamma represents higher effective friction and therefore a lower velocity by $1/\gamma$.

Force acting on the particle

$$\frac{d}{dt}r(t) = -\underbrace{\frac{1}{\gamma}}_{\text{Particle friction coefficient}}\boxed{\frac{d}{dr}U(r)} + \underbrace{\xi(t)}_{\text{White noise term}}$$

We know, in general, that the derivative of a potential energy function with respect to a position yields the negative force function. Using this, we can realise that it is possible to represent the force acting on our particle using the particle's potential energy function. This is evident in our equation as the derivative of the particle's potential energy at a given position, with the negative term on the outside.

Finally, we have our mysterious *Xi* component added onto the end, which represents the white noise properties (or simulated Brownian motion) of our instantaneous velocity. This is caused by the random collisions experienced by the particle from the fluid surrounding it, and therefore means the force at one instant is entirely unrelated to the force at another instant, resulting in an inability to be expressed by standard functions. However, we can represent this in another form as the square root of 2D times a new white noise function $W(t)$, where we now have an introduced influence of a 'diffusion tensor' (D) on the velocity generated by this stochastic term.

When the equation above is approximated, we can then model this difficult-to-represent white noise term with a random variable drawn from a Gaussian probability distribution, where we have [1]:

$$x_i = x_{i-1} - \frac{K_y}{\gamma}x_{i-1}\Delta t + \sqrt{2D\Delta t}w_{x,i}$$

Now, there is a relation of each iteration to time, which is much more suitable for code.

In our new equation, we now have the x-position at the current timestep expressed relative to its value at the previous timestep (i-1). Our new force equation can be seen as having a stiffness represented by Ky from the previous timestep, with a change in time. Although we still represent the white noise term as w, we now have this Gaussian randomized variable sampled at discrete timesteps. Still, the term that has remained constant for both equations is the Diffusion Tensor D.

OBJECT GEOMETRY

The diffusion tensors for a circle, an oval, and an arbitrary shape are listed below.

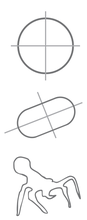

Your paragraph text

$$D_{\text{circle}} = \begin{pmatrix} D & 0 & 0 \\ 0 & D & 0 \\ 0 & 0 & D_\theta \end{pmatrix}$$

$$D_{\text{oval}} = \begin{pmatrix} D_x & 0 & 0 \\ 0 & D_y & 0 \\ 0 & 0 & D_\theta \end{pmatrix}$$

$$D_{\text{arbitrary}} = \begin{pmatrix} D_x + r_y^2 D_\theta & -r_x r_y D_\theta & -r_y D_\theta \\ -r_x r_y D_\theta & D_y + r_x^2 D_\theta & r_x D_\theta \\ -r_y D_\theta & r_x D_\theta & D_\theta \end{pmatrix}.$$

A circle is perfectly symmetrical along any axis, so its translational diffusion coefficient is the same in both the x- and the y-direction, and the rotational motion does not couple to its translational motion. Similarly, in an oval where the center of diffusion is not offset from the center of mass, rotational and translational motion do not couple to each other. However, since an oval does have x- and y-axes of unequal length, diffusion coefficients will be different in the x- and y-directions.

The diffusion tensor for an arbitrary shape introduces two new parameters: r_x and r_y, which represent the offsets between the center of diffusion and the center of mass in the x- and y-direction in the frame of reference of the particle. This offset results in coupling between rotational and translational diffusion.

$$dX_{body}(t) = \frac{1}{k_B T}D_{body}(\theta)F_{body}dt + \sqrt{2D_{body}}\,dW_{body}(t)$$

$R(\theta)$: Rotation matrix converting Body frame ↔ Lab frame.

The equation above shows how the diffusion tensor is incorporated into the general equation describing particle dynamics, where a rotation matrix is used to convert the diffusion tensor in the body frame to one observed in the lab frame.

BROWNIAN DYNAMICS OF ASYMMETRIC OBJECTS

Figure 2 below shows the plots returned when all trap and diffusion parameters are positive and definite, when an asymmetric object is considered (left), alongside the averaged Brownian trajectory from 100 runs under deliberately strong trap forces to make the drift toward the origin visible within a short simulation window (right).

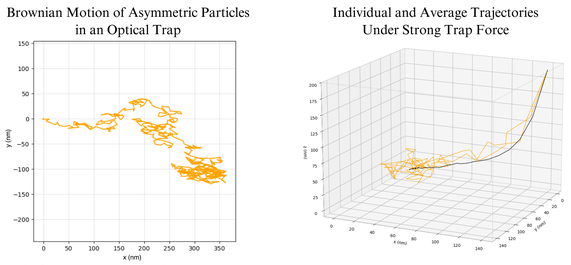

Fig 2: Brownian trajectory of an asymmetric particle; graphical demonstration of how two individual Brownian trajectories compare to the mean of 100 trajectories.

The arrows in Figure 3 below indicate the instantaneous offset between the center of mass and the center of diffusion. This offset rotates with the particle as it moves towards the center of the trap. Whenever a trap force acts on the particle, this "lever arm" converts part of the trap force into a torque, producing coupled translational and rotational motion. Figure 4 shows the limiting case where particle motion is purely deterministic due to trap forces acting on it. This forms the basis for our regression-based approach for estimating tensor entries under trapped conditions.

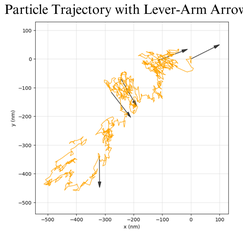

Fig 3: Trajectory of a particle with instantaneous COM-COD offset represented as lever-arm arrows.

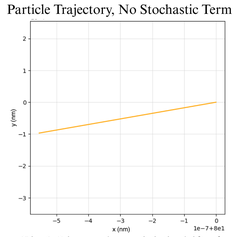

Fig 4: Linear, deterministic drift of an asymmetric particle

RESULTS

Using the parameters in Table 1 [2-7], we assigned each bacterium a normalized geometric complexity using the following equations:

$$Complexity = \sqrt{(\frac{D_x - D_y}{D_x + D_y})^2 + (\frac{r_x}{L})^2 + (\frac{r_y}{L})^2} \quad , \qquad C_{normalized} = \frac{C - C_{min}}{C_{max} - C_{min}}.$$

Name of Bacteria	Shape	D_x (m^2s^{-1})	D_y (m^2s^{-1})	D_θ (rad^2s^{-1})	r_x (m)	r_y (m)	L (m)	Normalized Complexity (0-1)
Coccus	Sphere	4.14E-15	4.14E-15	8.28E-15	No offset.	No offset.	1.00E-6	0.000
Bacillus	Rod	2.30E-13	1.80E-13	4.60E-02	2.35E-06	4.35E-07	5.00E-6	0.773
Vibrio Cholorae	Curved rod	6.05E-13	4.56E-13	6.78E-01	1.00E-06	1.50E-07	1.50E-6	0.912
Helicobacter Pylori	Helix	3.28E-13	2.43E-13	9.46E-02	2.00E-06	2.50E-07	3.25E-6	1.000

Table 1: Diffusion parameters and normalized geometric complexity for four bacteira.

Figure 5 below shows how covariance values change with bacteria of different geometries. It is worth noting that while *H. pylori* is geometrically more complex than *V. cholorae*, *x*-θ and *y*-θ couplings depend primarily on D_θ; *H. pylori*'s spiral shape increases surface area and hence rotational drag, which weakens its translational-rotational coupling despite its more complex geometry.

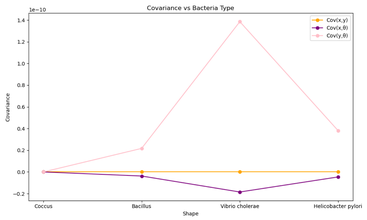

Fig 5: Covariance of x, y, and θ for different bacteria, using average trajectory over 100 runs.

Then, to estimate the entries of a particle's diffusion tensor based on information from its average trajectory under **free diffusion** conditions, we used the identity that on the interval [t,t+Δt],

$$D_{\text{lab}}(\theta) \approx \frac{\text{Cov}(\Delta X)}{2\,\Delta t}$$

which assumes that at small Δt, particle motion is purely stochastic [9]. In an optical trap with trap stiffness $\kappa_x = \kappa_y = 1.00\times10^{-6}$ Nm^{-1}, the estimation uses the Ornstein-Uhlenbeck process [1,8], where A is the linear regression matrix obtained by rearranging the OU equation:

$$\Delta X_n \;=\; A X_n \,\Delta t \;+\; \sqrt{2D\,\Delta t}\,\xi_n, \qquad \xi_n \sim \mathcal{N}(0,1).$$

Figure 6 below shows how RMS percentage error increases with geometric complexity. The trend differs from Figure 4 as estimation error is mainly influenced by the particle's COM-COD offset, which amplifies noise in the regression.

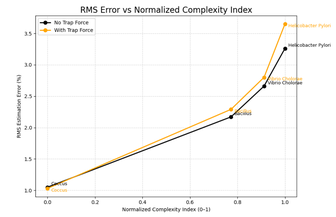

Fig 6: Graph of RMS of percentage error of estimated tensor entries against normalized geomrtric complexity.

CONCLUSION

Our results show that estimating particle geometry from Brownian dynamics is possible, but becomes less reliable for more complex geometries, confirming that asymmetry is a limiting factor in this estimation approach. Interestingly, introducing an optical trap presents a tradeoff: while the trap confines motion and facilitates data collection in an experimental setting, it also suppresses stochastic fluctuations and superimpose deterministic forces, which makes diffusion-based estimations less representative of the particle's geometry at higher stiffness values.

Having established that Brownian trajectories encode geometric information, future work could extend this model to three dimensions, where axial offsets may introduce new coupling effects. Another direction is to test whether trajectories are uniquely tied to a particle's shape, or if distinct geometries can produce indistinguishable motion.

REFERENCES

[1] Jones, P.H., Maragò, O.M. and Volpe, G. (2015) *Optical Tweezers: Principles and Applications*. Cambridge: Cambridge University Press.
[2] De la Torre, J. G. (1984) 'Dimensions of rodlike macromolecules', *Biopolymers*, Vol 23, 611-615.
[3] Milo, R. et al. (2010) 'BioNumbers database', *Nucleic Acids Research*, 38(s1), pp. D750–D753. BNID 100212.
[4] Pönisch, W. (2018) 'Computational model of bacterial motility and mechanics', *Dynamics of bacterial aggregates – theory guided by experiments*. PhD thesis, TU Dresden / Max Planck Institute for the Physics of Complex Systems.
[5] Qi, K. et al. (2025) 'Unravel the rotational and translational behavior of a single squirmer in flexible polymer solutions at different Reynolds numbers', *Communications Physics*, 8(1), p. 487.
[6] Dubay, M.M., et al. (2022) 'Quantification of Motility in *Bacillus subtilis* at Temperatures Up to 84°C Using a Submersible Volumetric Microscope and Automated Tracking', *Front. Microbiol.*, 13, 836808. doi:10.3389/fmicb.2022.836808.
[7] IARC Working Group (2012) 'Helicobacter pylori', in *Biological Agents* [online]. Lyon (FR): International Agency for Research on Cancer. pp. 381–414. (IARC Monographs on the Evaluation of Carcinogenic Risks to Humans, No. 100B).
[8] Lalley, S. (2008) *Brownian Motion* [online]. University of Chicago lecture notes.